Reactions of Sodium Clusters with Oxygen Molecules

L. Bewig,† U. Buck,* S. Rakowsky,‡ M. Reymann,§ and C. Steinbach

Max-Planck-Institut für Strömungsforschung, Bunsenstrasse 10, D-37073 Göttingen, Germany

Received: March 3, 1997; In Final Form: April 25, 1997[⊗]

In a crossed molecular beam experiment, the reactive scattering of sodium clusters Na_n ($n \leq 33$) with molecular oxygen O_2 is investigated. By measuring the angular and the velocity distributions of the scattered reaction products, direct information on the reaction mechanisms is obtained. The sodium clusters are generated in a supersonic expansion of sodium vapor from an oven with a refilling system with argon carrier gas. The products are detected by photoionization at a wavelength of 308 nm and mass analyzed in a time-of-flight mass spectrometer (TOF-MS). In addition, a fast chopper with a pseudorandom sequence modulating the sodium cluster beam allows us to determine at the same time the velocity distributions of the products. The scattering of Na clusters with O_2 shows two series of reaction products. The monoxides Na_nO are centered around Na_3O with $2 \leq n \leq 5$, while the metal-rich dioxides Na_nO_2 are detected for $3 \leq n \leq 32$ with varying intensities and a maximum at Na_5O_2. For all products, the measured angular and velocity distributions exhibit forward scattering with a large fraction of the reaction energy deposited into internal excitation of the products. This is in agreement with the classical harpooning model. The general result is explained by the energetic stability of the product complexes.

1. Introduction

Alkali-metal clusters belong to the best studied systems with respect to their electronic structure and optical properties.[1] In contrast, the chemical reactivity which is at least equally important for understanding surface reactions on metals is much less investigated. Notable exceptions are the reactions of alkali-metal clusters with oxygen. Most of them are conducted in flow reactors or gas aggregation cells by measuring the abundance pattern or ionization potentials in mass spectrometers.[2] In this way, the stability of doped oxides of the kind $Cs(Cs_2O)_n$[3] and $Li(Li_2O)_n$[4] was established. Large sodium clusters with filled electronic shells were found to be unreactive.[5] In all these experiments, the two reactants are not very well-defined, and it is difficult to relate them to the measured products. In a beam-scattering cell arrangement, the integral cross sections of Na_n clusters with O_2 have been measured for $n \leq 40$.[6] For the explanation of the relatively large cross sections, the authors invoked a charge transfer model. In a crossed-beam arrangement, the integral cross sections for chemiionization were measured in the reactions of Na_n with O_2 in the range $4 < n < 11$.[7] Primarily, the ions $Na_5O_2^+$ and Na_3O^+ were found. In a further experiment, the differential scattering cross sections of the neutral products generated in Na_n ($n \leq 8$) + O_2 collisions were found to be Na_nO ($n \leq 4$) and Na_nO_2 ($n \leq 6$).[8] Based on the large cross sections and the measured angular distributions which are all peaked in the forward direction, the authors speculate that the harpooning model is operating. Based on statistical estimates of the lifetimes of the formed complexes, they conclude that the monoxides are produced in direct reactions, while the dioxides result from highly excited complexes.

Only the last experiment is in the tradition of the classical crossed-molecular-beam work pioneered by Herschbach[9] and Lee[10] in which the reaction mechanisms are deduced from a careful measurement of the angular and the velocity distributions of the reaction products. In that respect, there is still one component missing in the experiment of Goerke *et al.*,[8] namely, the simultaneous measurement of the translational energy of the products. In the present paper, we describe and analyze such a complete experiment for the scattering of $Na_n + O_2$ over a much larger size range, $n \leq 33$. We find two types of products. The monoxides Na_nO are centered around Na_3O with $2 \leq n \leq 5$, while the metal-rich dioxides Na_nO_2 are detected for $3 \leq n \leq 32$ with Na_5O_2 as the product of largest intensity. For more than 15 of these products, we measured the angular and the velocity distributions. For that purpose, our crossed-molecular-beam machine had to be changed. It was originally built to measure the fragmentation upon electron impact of sodium clusters which are size-selected by scattering from a helium atom beam.[11] In order to make the detection of a large number of products of a chemical reaction feasible, we replaced the quadrupole mass filter by a time-of-flight mass spectrometer (TOF-MS) which allows us to measure, at the same time, the velocity by time-of-flight analysis using the pseudorandom chopping technique.[12] In this way, we get all the products in one measurement together with their velocity. The remaining question of the specification of the reactants which start as a distribution can partly be answered by the kinematic and energetic constraints of this well-defined experiment. Energetically most of the cluster reactions are exothermic so that a large amount of energy has to be distributed in the reaction. Calculations of the product molecules are available for some sodium monoxide clusters[8,13] and stoichiometric lithium oxide clusters of the type $Li_{2n}O_n$.[14]

The reaction of sodium atoms with oxygen molecules is endothermic in the ground state. Upon electronic excitation to the 4D state, strong backward scattering of the NaO product was observed.[15] This implies that either a very restricted collinear geometry[16] and/or the coupling to a charge-transfer state with electronically excited O_2^- is operating.[17]

* Corresponding author.
† Present address: Auer SOG Glaswerke, Hildesheimer Str. 39, D-37581 Bad Gandersheim, Germany.
‡ Present address: Robert-Rössle-Klinik, OP 2000, Lindenberger Weg 80, D-13122 Berlin, Germany.
§ Present address: Institut für Physik der Technischen Universität, D-09107 Chemnitz, Germany.
⊗ Abstract published in *Advance ACS Abstracts,* July 1, 1997.

S1089-5639(97)00785-8 CCC: $14.00 © 1997 American Chemical Society

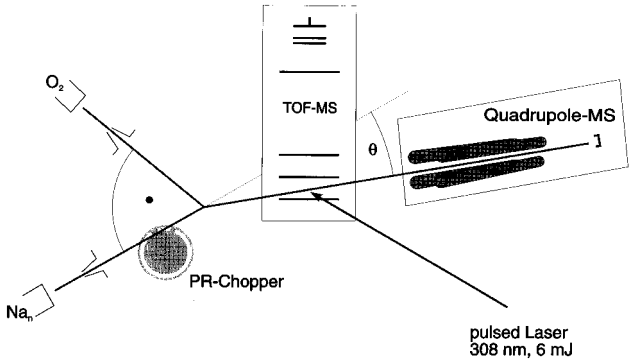

Figure 1. Schematic view of the experimental setup.

The emphasis of the present experiment will be on the elucidation of the reaction mechanism, the distribution of the energy, and the size dependence of the sodium cluster oxidation. We start with a short description of the experimental setup in section 2, present the results in section 3, and discuss the implications in section 4.

2. Experiment

The experiment was performed in a universal crossed-molecular-beams machine which is described elsewhere.[11,18] The sources and detection schemes used in this work are shown in Figure 1. Briefly, a seeded supersonic cluster beam was crossed at 90° with a supersonic O_2 beam in a vacuum chamber under single-collision conditions. The scattered products were resolved and detected by a TOF-MS applying pulsed UV-laser photoionization.[12] The ionization region is located 37.4 cm downstream from the collision region. Alternatively, a quadrupole mass spectrometer equipped with an electron-bombardment ionizer was used for the velocity analysis of the direct beams. Both detectors could be rotated in the plane defined by the sodium and oxygen beams, enabling us to measure the product angular distributions in an angular range from −3° to 92° with respect to the cluster beam.

We note that the TOF-MS is of crucial importance for the detection of the product masses. In cluster reactions, they are usually unknown in advance, and in our arrangement, we get them all within one sequence. In addition, the measurement of the mass information was coupled to the measurement of the velocity distributions of the products using a fast mechanical chopper (1000 Hz) with a pseudorandom (PR) sequence modulating the sodium cluster beam. By detecting the masses in each channel of the pseudorandom sequence and a subsequent deconvolution of the two-dimensional array of mass and velocity information, we simultaneously measure the TOF distributions for all products.[12]

The sodium cluster source and the liquid metal refilling system have been described by Bewig *et al.*[19] The sodium clusters were generated in a supersonic expansion of sodium vapor from an oven heated to 780 °C with 2−3 bar of argon carrier gas. To obtain a stable cluster beam, the 120-μm diameter nozzle was kept at a temperature sufficiently higher than the oven, typically at 840 °C. Under these conditions, sodium clusters Na_n with $n \leq 33$ were produced and the yield of the large Na_n clusters slightly increased compared to an operation of the nozzle at 865 °C. The O_2 beam was formed in the expansion of neat O_2 gas at a pressure of 38 bar through a 30-μm nozzle at room temperature. Signals of clusters could not be detected at the mass spectrometer. In a different experiment, we measured the fragmentation probability of oxygen dimers, which is large but smaller than 1, so that the missing signal indicates that the beam is free of clusters.[20] The velocities of the beams were 722 ms^{-1} for O_2 and between 1125 ms^{-1} for Na_3 and 1051 ms^{-1} for Na_{19}. The collision energies ranged between 0.202 and 0.255 eV depending on the cluster size. The beam data of some selected clusters are sampled in Table 1.

TABLE 1: Measured Laboratory Velocities, Collision Energies, and Laboratory Angles of the Center of Mass for the Clusters Na_n ($3 \leq n \leq 20$)

n	velocity m/s	collision energy, meV	angle, deg
3	1125	202	16.6
4	1108	215	12.8
5	1112	228	10.2
6	1119	239	8.5
7	1104	241	7.4
8	1099	244	6.5
9	1084	244	5.9
10	1091	249	5.3
11	1072	246	4.9
12	1084	252	4.4
13	1068	249	4.1
14	1077	254	3.8
15	1069	253	3.6
16	1073	255	3.4
17	1059	252	3.2
18	1060	253	3.0
19	1051	251	2.9
20	1061	255	2.7

For the photoionization of the products at an ionizing wavelength of 308 nm, an excimer laser (Lambda Physics EMG 103 MSC) has been used. By a mirror fixed at the rotating detector unit, the excimer laser radiation was steered into the ionizing volume of the TOF-MS independent of the actual detector position. The excimer laser was operated at a repetition rate of 70 Hz for the measurement of the velocity distributions and the pulse energy at the ionizing volume adjusted by a focusing lens with 1000-mm focal length to 6 mJ, corresponding to a flux of 12 mJ/cm^2. Later, a Nd-YAG laser (Quantel-Brillant) with a maximum repetition rate of 50 Hz was used for photoionization at 266 and 355 nm. The compact laser head was directly fixed at the detector unit, allowing us an easier alignment of the laser output into the ionizing volume. To avoid multiphoton ionization, the Nd-YAG laser output has been attenuated by a telescope to 6 mJ of pulse energy.

Product-size distributions have been compared at ionizing laser wavelengths of 193, 266, 308, and 355 nm. The product angular distributions have been measured at 308 and 355 nm, respectively, while the ionizing laser wavelength for product velocity distributions was 308 nm, exclusively. The choice of these wavelengths makes sure that the ionization takes place by single photons. This is also confirmed by the measured linear fluence dependence.

3. Results and Analysis

The scattering of Na_x clusters with O_2 results in the formation of monoxide Na_nO and dioxide Na_nO_2 clusters as reaction products. For the discussion, the reaction equations for a direct reaction with these two reaction products read

$$Na_x + O_2 \rightarrow Na_nO + Na_{x-n}O + \Delta D \quad (1)$$

$$Na_x + O_2 \rightarrow Na_nO_2 + Na_{x-n} + \Delta D \quad (2)$$

The reaction energies ΔD are known for a number of reactions, namely, $x = 2$, 3, 4, 5, and 8, from the calculated binding energies of the products.[8] Because of the size distribution in the Na_x cluster beam, the reactant Na_x leading to a specific product Na_nO or Na_nO_2 is not known a priori from the

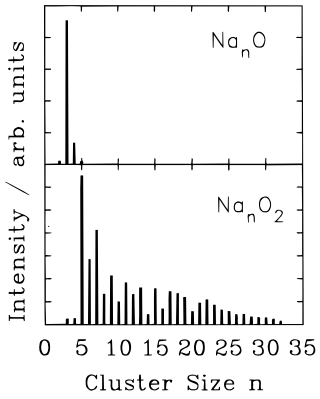

Figure 2. Product distribution as a function of cluster size measured at 3° laboratory angle by photoionization with 308 nm.

experiment. From indirect conclusions which will be discussed later, $x = n + 2$ turned out to be a good assumption.

In Figure 2, the product ion intensities from a TOF mass spectrum recorded at a laboratory scattering angle of 3° with an ionizing laser wavelength of 308 nm are displayed. This angle corresponds, as we will see later, to a position not too far away from the maximum intensity for all cluster sizes measured. We observe a short series of monoxides Na_nO ($2 \leq n \leq 5$) centered around the main product Na_3O and a long series of dioxides Na_nO_2 ($3 \leq n \leq 32$) with a maximum at $n = 5$ and alternating intensities up to $n = 17$ and a minimum at $n = 20$. Nonreactively scattered sodium clusters are also observed in the TOF mass spectrum at 3°, the dominant Na_3 having similar intensity as Na_3O and Na_5O_2, respectively. For the larger clusters, $20 \leq n \leq 32$, the reactive signals are larger than the nonreactive ones. Clearly, sodium dioxides Na_nO_2 are formed with a large reaction cross section in the whole range of reactants Na_n, while the formation of monoxides is restricted to small reactants.

For a correct interpretation of the data, we have to take into account the ionization process. Experimentally, we used different laser wavelengths to shed some light onto this problem. Compared with the product ion intensities in Figure 2, ionization with 266 and 193 nm results in increased intensities (relative to the intensity of Na_3O) for Na_2O, Na_2O_2, Na_3O_2, and Na_4O_2 but decreased intensities for the dioxides larger than Na_7O_2. In the case of Na_2O, this can be rationalized by the increase in the photoionization efficiency (PIE). Na_2O has an ionization potential (IP) between 4.45 ± 0.03[21] and 5.06 ± 0.4 eV,[2] which cannot be reached with one photon at 308 nm and is just reached with 266 nm. Likely the IP for the smaller dioxides is increased compared to the larger ones, leading to the observed increase of the PIE at shorter ionization wavelengths. Unfortunately, it is impossible to detect the product NaO, since the ionization potential of 7.1 eV[22] cannot be reached using 193 nm (6.43 eV). The reduction of product ion intensities for the larger dioxides observed at shorter ionization wavelengths is apparently caused by an increasing fragmentation of these products at higher excess energy. The product intensities taken at 355 nm show the same behavior as those of Figure 2.

The ion signals for Na_nO_2 ($4 \leq n \leq 17$), and to a lesser extent also for Na_nO, show a pronounced odd−even alternation present with all ionizing laser wavelengths, the signal for ions containing an odd number of Na atoms being more intense than the signals for the even-numbered neighbors. The ionization efficiency can be ruled out as a possible reason, since several products have the same IP's like Na_3O and Na_4O with 3.9 eV,[2] but totally different product intensities. It has been argued[8] that the ion stability might be the reason for a higher stability of the odd-numbered cluster ions with an even number of electrons against fragmentation caused by excess energies. We note that in our measurement at 355 nm, for which the excess energy for most of the clusters is very small, the even−odd effect is still present. Therefore, we attribute this effect to properties of the neutral cluster products.

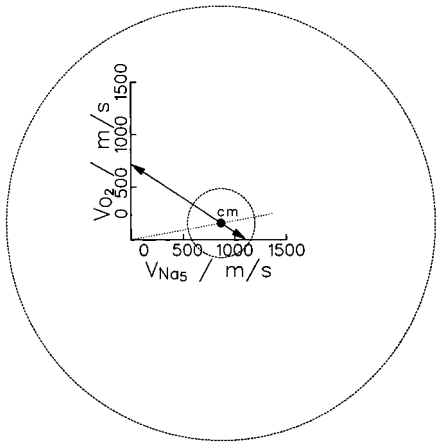

Figure 3. Newton diagram for the reaction $Na_5 + O_2$ at a collision energy of 0.228 eV. The large circle stands for the maximum center-of-mass recoil velocity of the Na_3O product. The small circle indicates the center-of-mass recoil velocity observed in the experiment.

A typical, most probable Newton diagram is shown in Figure 3 for the reaction

$$Na_5 + O_2 \rightarrow Na_3O + Na_2O + \Delta D \qquad (3)$$

This reaction is exothermic with a reaction energy $\Delta D = +4.22$ eV, and the collision energy in the center-of-mass frame is 0.228 eV in our experiments. The large Newton circle drawn in Figure 3 describes the possible velocities of the product Na_3O for zero internal excitation of the products or maximum center-of-mass recoil velocity. The small circle stands for an appreciable internal excitation or small translational energies. The values correspond to the experimental results (see the later discussion). The alternative reaction for the same product, $Na_4 + O_2 \rightarrow Na_3O + NaO + \Delta D = 2.2$ eV, leads to a similar Newton diagram as do the diagrams for the sodium dioxide products.

The laboratory angular distributions for the products Na_3O, Na_5O_2, Na_7O_2, and $Na_{11}O_2$ are shown in Figure 4. The angular range covered in the measurements is between −3° and +60°. Similar looking angular distributions have been obtained also for the larger dioxides up to $Na_{21}O_2$. No data could be recorded between −1° and +1° because of detector saturation effects close to the direct sodium cluster beam. Clearly, the maximum of the angular distributions falls in the forward direction for all the products. The product angular range is narrow compared to the maximum scattering angle at the available reaction energy. With increasing energy, the distribution becomes narrower. The maximum angles at which products have been detected are 12° for Na_2O, 45° for Na_3O, 15° for Na_4O, 23° for Na_5O_2, 15° for Na_6O_2, 15° for Na_7O_2, and 10° for Na_8O_2. Uniformly, all investigated products of the reaction of Na_x with O_2 are forward scattered with respect to the Na_x cluster beam.

The narrow product angular range indicates the formation of highly internally excited reaction products with only a small fraction of the available energy in translation. The angle which corresponds to the center-of-mass for reactants from Na to Na_{13} with O_2 varies from +41.0° to +3.9°. This value is definitely outside the range of the measured maximum intensities of the angular distributions of all products. Thus, the formation of a long-lived collision complex exhibiting angular distributions

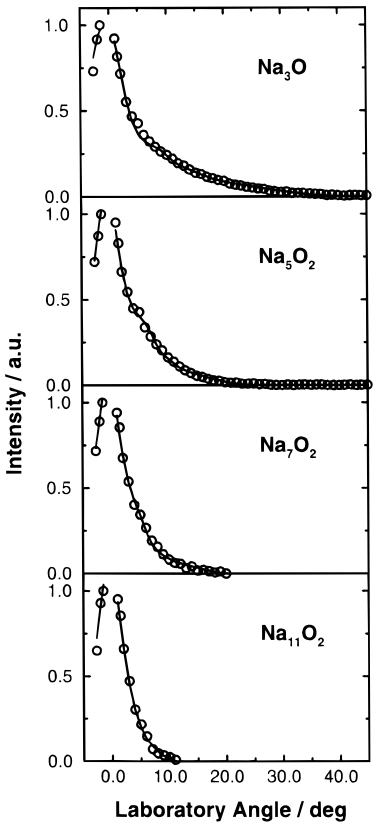

Figure 4. Laboratory angular distribution for different products measured at 308 nm. The solid line represents the distribution calculated with the best-fit center-of-mass distributions of Figures 8 and 9.

with a forward−backward symmetry or an association reaction with a maximum of the angular distribution at the center-of-mass angle can be excluded for the reaction of Na_x with O_2. Angular distributions recorded with 355 nm show the same features.

Product time-of-flight distributions have been measured at laboratory scattering angles between −2.7° and +15°. Figures 5, 6, and 7 depict the time-of-flight distributions of Na_3O, Na_5O_2, and $Na_{11}O_2$ at different laboratory angles. As for the angular distribution, the velocity distribution of Na_3O (speed ratio = 4.6 at −2.7°) is slightly broader than the velocity distribution of the dioxides (Na_5O_2: speed ratio = 6.6). The velocity distributions of the larger dioxides narrow even further with increasing mass. The laboratory velocity at the maximum of the velocity distribution turns out to be almost constant for all measured laboratory angles, and it is with 1110 m/s for the two products Na_3O and Na_5O_2 identical within 2% with the sodium cluster velocity.

For the interpretation, the laboratory angular and velocity distributions (Θ,v) have been transformed to the center-of-mass coordinate (θ,u) frame by $I_{lab}(\Theta,v) = I_{cm}(\theta,u)v^2/u^2$. Because of the finite resolution of the experiment, the analysis of the laboratory data is carried out by a forward convolution over the experimental conditions of trial center-of-mass product flux distributions of angle and translational energy E' of the form

$$I_{cm}(\theta,E') = T(\theta)P(E') \qquad (4)$$

The angular and velocity divergences of the beams, the finite scattering volume, and detector dimensions are all accounted for. The continuous lines in Figures 4−7 are calculated from the best-fit center-of-mass distributions which are depicted as solid lines in Figure 8 for Na_3O and in Figure 9 for Na_5O_2,

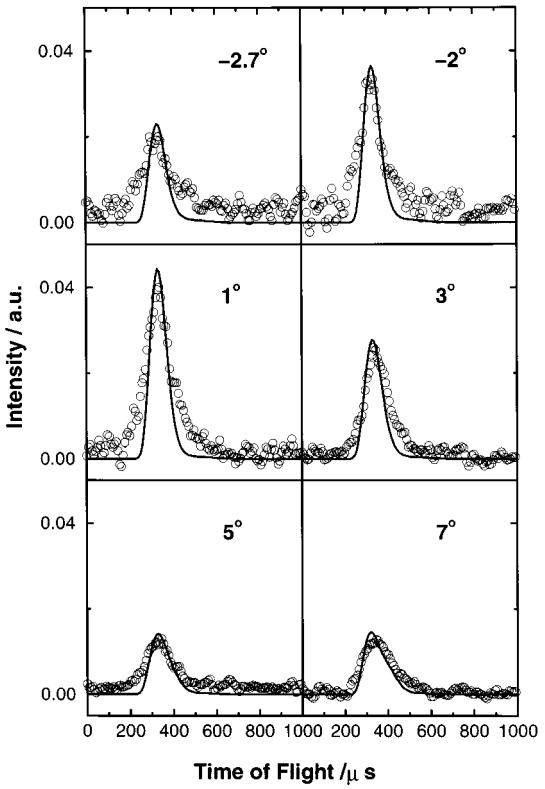

Figure 5. Time-of-flight data of Na_3O for indicated laboratory angles. Open circles represent the experimental data; the solid line represents the distribution calculated with the best-fit center-of-mass distributions of Figure 8.

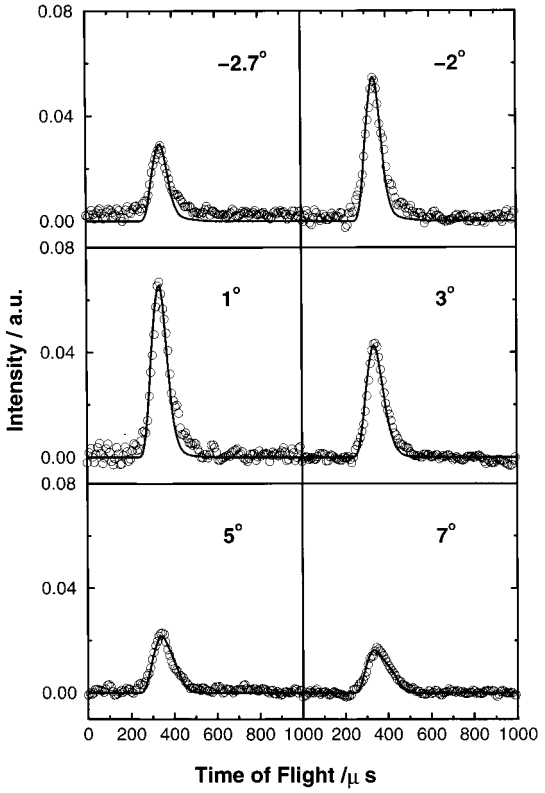

Figure 6. Time-of-flight data of Na_5O_2 for indicated laboratory angles. Open circles represent the experimental data, the solid line the distribution calculated with best-fit center-of-mass distributions of Figure 9.

Na_7O_2, and $Na_{11}O_2$. The averaged translational energy release is presented in Table 2 together with the reaction and the collision energies.

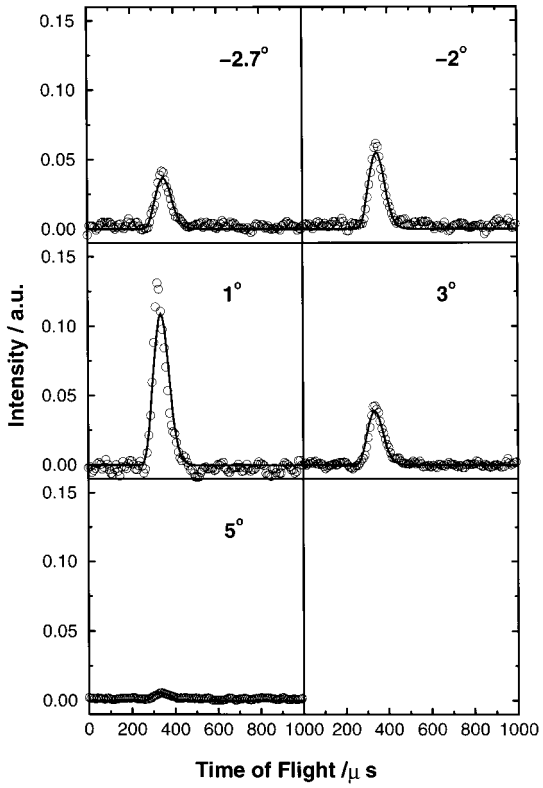

Figure 7. Time-of-flight data of $Na_{11}O_2$ for indicated laboratory angles. Open circles represent the experimental data; the solid line represents the distribution calculated with the best-fit center-of-mass distributions of Figure 9.

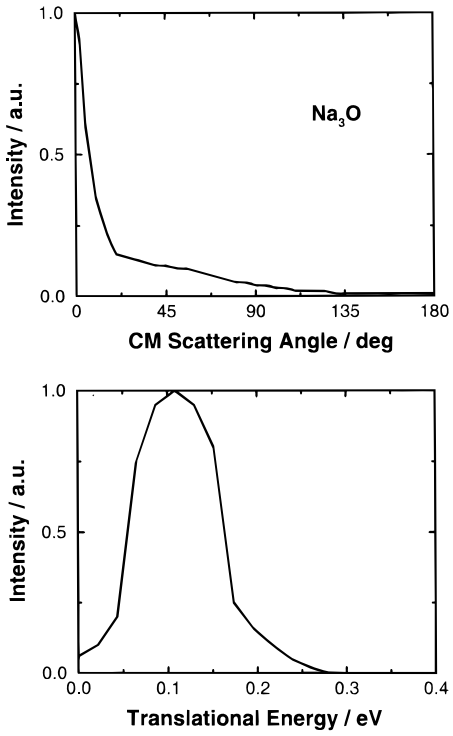

Figure 8. Center-of-mass product angular and translational energy distributions for the indicated reaction products from the reaction $Na_5 + O_2$.

The center-of-mass angular distributions $T(\theta)$ exhibit all a strong forward scattering with a tail which dies out at about 135° for the dioxides and continues to 180° for the monoxides with a value of 0.01. There are some slight differences in the width which is larger for the larger clusters. However, no distinct differences between the angular distributions of the

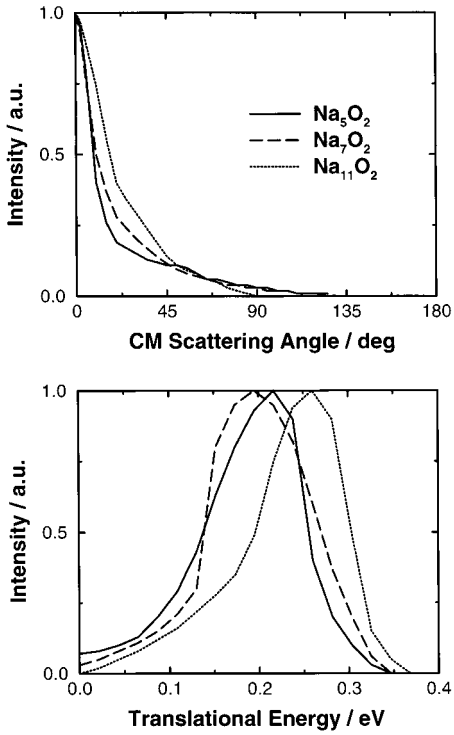

Figure 9. Center-of-mass product angular and translational energy distributions for the indicated reaction products Na_nO_2 from the reaction $Na_{n+2} + O_2$.

monoxides Na_nO ($2 \leq n \leq 5$) and all the dioxides have been found that would indicate a different reaction mechanism for these species as reported in ref 8.

The center-of-mass translational energy distributions again exhibit the same behavior for all products. In spite of the large exothermicity of the reaction in the range of 4 eV, only a very small amount of energy is found in the translational recoil of the product. For the dioxide clusters, it is about 0.2 eV, which roughly corresponds to the collision energy. In case of the monoxides, it is with 0.1 eV only half of it. These findings suggest that nearly all the available energy goes into internal excitation of the product.

4. Discussion

The measured angular and energy distributions clearly indicate forward scattering and nearly complete internal excitation of the reaction products. These are typical ingredients of the harpooning-type reactions with a long-range electron transfer from the Na_x cluster to the O_2 molecule in the entrance channel at large impact parameters followed by a mutual reactive approach of the ionic components Na_x^+ and O_2^-.[23] Because of the large exothermicity of these reactions, the metal-rich product cluster oxides are highly internally excited.

While the reaction of the monomer with O_2 is endothermic and only occurs after electronic excitation with product intensities in the backward direction, the clusters provide an environment for much better energetics and a facile electron transfer. We note that both the angular and the velocity distributions are quite narrow. The pronounced forward scattering in the direction of the cluster is obviously connected with the large impact parameters at which the electron transfer occurs, thus indicating a direct reaction. In contrast to the usual spectator model, however, like in the typical reaction $K + Br_2$ in which the forward scattering of the ionic bound product, say KBr, is caused by the backward scattering of the spectator, say Br,[24] the products of the present experiment consist mostly of the

reacting clusters and the molecule (dioxides) or the O atoms are split between the two products (monoxides). In both cases, there are no spectators.

The other interpretation, that of a complex-forming reaction, seems to be ruled out by the quite narrow angular and velocity product distributions, which do not show up near the center-of-mass angle. In addition, we do not find any remarkable intensity at $\theta = 180°$ which would be an indication of an oscillating complex in case the lifetime is comparable to the rotational period of the complex. Nevertheless, it is still possible that the backward scattered peak is totally suppressed by the very short lifetime of the many-dimensional complex in comparison to the rotational period.

Our measured angular distributions agree quite well with those published by Goerke *et al.*[8] for the two main products Na_3O and Na_5O_2, as does our conclusion that the harpooning mechanism is operating. We do not find, however, any serious difference between the dioxides and the monoxides concerning the reaction mechanisms as they postulate. The large internal energy of the products observed in these experiments makes it quite plausible that this energy can lead to chemiionization, as was found recently[7] with the maximum intensity for the same two cluster sizes, namely Na_3O and Na_5O_2.

Now we would like to address the question of how to explain, at least in a qualitative way, the size dependence of the results. As was discussed earlier, we think that the intensities displayed in Figure 2 are mainly caused from the behavior of the neutral products. The general falloff of the intensity is certainly caused by the decreasing intensity of the reactants for $n > 8$. The detailed structure, however, should be a consequence of the stability of the products. According to statistical arguments, the most exoergic reaction path is always favored.[25] Therefore, the reaction energies ΔD are a key point in the further discussion. They have been calculated for products up to Na_5O_2 resulting from reactants up to Na_8 using the reaction energies for specific reactants given in ref 8 and 13 and the dissociation energies of Na_x clusters[26] (see Table 3 in ref 8). We are aware of the problem that this calculation is only of restricted value because of its approximative character. In addition, the numbers for Na_5O_2 are mainly based on an educated guess rather than taken from a real calculation. Nevertheless, these data, at least, reproduce correctly the general trends, as is shown in a comparison with recent calculations for lithium oxides.[14,27] In spite of these drawbacks, we present here the results for the reactions which lead to the main products Na_3O

$$Na_3 + O_2 \rightarrow Na_3O + O \qquad \Delta D = 0.60 \text{ eV} \qquad (5)$$

$$Na_4 + O_2 \rightarrow Na_3O + NaO \qquad \Delta D = 2.35 \text{ eV} \qquad (6)$$

$$Na_5 + O_2 \rightarrow Na_3O + Na_2O \qquad \Delta D = 4.22 \text{ eV} \qquad (7)$$

$$Na_6 + O_2 \rightarrow Na_3O + Na_3O \qquad \Delta D = 5.08 \text{ eV} \qquad (8)$$

$$Na_7 + O_2 \rightarrow Na_3O + Na_4O \qquad \Delta D = 6.85 \text{ eV} \qquad (9)$$

and Na_5O_2

$$Na_6 + O_2 \rightarrow Na_5O_2 + Na \qquad \Delta D = 4.20 \text{ eV} \qquad (10)$$

$$Na_7 + O_2 \rightarrow Na_5O_2 + Na_2 \qquad \Delta D = 4.30 \text{ eV} \qquad (11)$$

$$Na_8 + O_2 \rightarrow Na_5O_2 + Na_3 \qquad \Delta D = 3.70 \text{ eV} \qquad (12)$$

If we compare the reaction energies, we observe two different trends. For the monoxides, the exothermicity increases with increasing sodium cluster size, while for the dioxides these values decrease. The same trends are found for other product molecules but with different absolute values. For the product Na_2O, the reaction energies range from -0.92 to 2.94 eV with the reactants Na_2 to Na_4 and for the product Na_4O from 2.19 to 8.33 eV with the reactants Na_4 to Na_8. For the dioxides, we get the following results: 0.57−0.06 eV for Na_2O_2 (Na_3-Na_8), 1.75−1.12 eV for Na_3O_2 (Na_4-Na_8) and 3.16−2.53 eV for Na_4O_2 (Na_5-Na_8). The respective reactants are indicated in parentheses. The large increase of ΔD with increasing reactant size for the monoxides stems from the fact that the second product is also a monoxide whose binding energy increases in steps of 1.5−2.0 eV.[27] For the dioxides, in contrast, only the weaker changes in the bonding energies of the sodium clusters have to be taken into account.

TABLE 2: Collision Energies, Reaction Energies, and Averaged Translational and Internal Energies of the Products for Some Reactions (All Energies in eV)

product	reactant	E_{col}	ΔD	$\bar{E}'_{tr}$	$\bar{E}'_{int}$
Na_3O	Na_4	0.215	2.350	0.192	2.373
Na_3O	Na_5	0.228	4.220	0.111	4.337
Na_5O_2	Na_7	0.241	4.300	0.186	4.355
Na_7O_2	Na_9	0.244		0.196	
$Na_{11}O_2$	Na_{13}	0.246		0.228	

In order to get the most favored products, the reaction energy should be as large as possible with the constraint that the products themselves should not dissociate. An optimum value for this energy is around 4.0 eV. Under the assumption that this energy is equally distributed among the two products, the remaining 2 eV just corresponds to typical dissociation energies of the products. Based on this criterion, we immediately understand why, for smaller Na_x clusters, the monoxides dominate and, for larger reactants, only dioxides are found. The maximum for Na_3O results from the fact that for the product Na_2O, the reaction energies are too low and for Na_4O these values are too high. The values of the dioxides Na_2O_2, Na_3O_2, and Na_4O_2 are all too small to compete with the product Na_5O_2.

The two main product clusters Na_3O and Na_5O_2 are stable molecules both of the type $Na(Na_2O)_m$ with $m = 1$ and 2. The structure of Na_3O is a triangle of Na atoms with the O atom in the center[8,13] with one of the largest bonding energies per atom of this series. For the dioxides, only the smallest ones have been calculated[8] so that we do not know the structure of Na_5O_2 explicitly. The resulting structures for the smaller ones clearly show that the O atoms usually form strong bonds with their nearest alkali-metal atom neighbors.[14] Very probably this trend is continued for Na_5O_2.

These criteria can also be used for deciding which reactants lead to one specific product. In the case of Na_3O, the optimal value is only reached for reaction 7. In the case of Na_5O_2, the two equations (10) and (11) are equally probable. In principle, this question can be answered experimentally, if the second product is also measured. The search can be narrowed down to a limited angular range from the knowledge of the center-of-mass velocity flux distribution of the first product. We have conducted these measurements for reactions 7 and 8. The laboratory angular range which corresponds to the center-of-mass range of 180° is $\Theta_4 = 43.4° \pm 12°$ for (7) and $\Theta_4 = 28.6° \pm 8°$ for (8). The detector was moved to these laboratory angles Θ_4 and mass spectra were taken every couple degrees in the given angular range using the 193 nm of an ArF eximer laser for ionization. With this laser wavelength, also the small sodium monoxides except NaO can be ionized. No products at the masses of Na_2O or Na_3O have been detected over the whole range. The experiments were hampered, however, by the low laser fluence of 0.6 mJ. In addition to these laser

problems, there exists also the possibility that the internal excitation of the second product is larger than the dissociation energy.

Judging from the above discussion on the product intensities and the decreasing densities of Na_x in the reactant beam with increasing x, the reaction equations can be best interpreted by $x = n + 2$ for the production of Na_3O (see (1)) and by $x = n + 2$ or $n + 1$ for the dioxides (see (2)). Regardless of the remaining ambiguity in the reactant, we observe highly internally excited products as derived from the comparison of the product kinetic energy distribution to the available reaction energies.

5. Summary

The reaction of sodium clusters in the size range $n \leq 33$ with oxygen molecules is investigated in a crossed-molecular-beam experiment. By measuring the angular and velocity distributions of the products, complete information on the reaction mechanisms is obtained. We find two types of reaction products. The monoxides Na_nO are centered around Na_3O with $2 \leq n \leq 5$, while the metal-rich dioxides Na_nO_2 are detected for $3 \leq n \leq 32$ with Na_5O_2 as the product of largest intensity. For both reaction products, we find strong forward scattering with a narrow central distribution and extended tails. In spite of the large exothermicity of these reactions of up to 4 eV, the translational energy distributions peak at 0.2 eV for the dioxides and 0.1 eV for the monoxides. Nearly all of the available energy goes into the internal energy of the products. These findings are in accord with the classical harpooning model. The reaction starts with an electron transfer from the cluster to the oxygen molecule in the entrance channel at large impact parameters followed by a mutual approach of the ionic components. The large excess energy is essentially found in the internally excited products which, for the dioxides, are mainly formed by an exchange of Na or Na_2 by O_2. In the case of the monoxides, two products of nearly equal masses are generated which fly apart in the forward and backward directions. This model, which is mainly based on a statistical energy redistribution, which, in turn, is quite fast here, will hopefully be proved or disproved in the future by a detailed calculation. For that purpose, additional measurements of the second products are necessary with better detection methods than those described here. Furthermore, the reaction rates and the kinetic energy release can be calculated starting from statistical methods. The general result is quite different from the monomer reaction. In that respect, the clusters provide a much better environment both for the energetics and the electron transfer.

Acknowledgment. This work was supported by the Deutsche Forschungsgemeinschaft and the European Community Network "Collision Induced Cluster Dynamics" No. CHRX-CT94-0643. It is a pleasure to dedicate this article to Yuan T. Lee, from whose pioneering work on chemical reactions we learned so much. We thank W. Maring for helpful assistance in the project and P. Casavecchia for providing us with the program for calculating the center-of-mass variables. We thank V. Bonačić-Koutecky for sharing her results on Li_nO clusters with us prior to publication.

References and Notes

(1) See several articles in: *Clusters of Atoms and Molecules I*; Haberland, H., Ed.; Springer: Berlin, 1995.

(2) Dao, P. D.; Peterson, K. I.; Castleman, A. W., Jr. *J. Chem. Phys.* **1984**, *80*, 563. Peterson, K. I.; Dao, P. D.; Castleman, A. W., Jr. *J. Chem. Phys.* **1983**, *79*, 777. Peterson, K. I.; Dao, P. D.; Farley, R. W.; Castleman, A. W., Jr. *J. Chem. Phys.* **1984**, *80*, 1780.

(3) Martin, T. P. In *Clusters of Atoms and Molecules I*; Haberland, H., Ed.; Springer: Berlin, 1995; p 357.

(4) Brechignac, C.; Cahuzac, Ph.; Carlier, F.; de Frutos, M.; Leygnier, J.; Roux, J. Ph. *J. Chem. Phys.* **1993**, *99*, 6848.

(5) Lange, T.; Göhlich, H.; Näher, U.; Martin, T. P. *Ber. Bunsenges. Phys. Chem.* **1992**, *96*, 1109.

(6) Kresin, V. V.; Scheideman, A. *J. Chem. Phys.* **1993**, *98*, 6982.

(7) Hampe, O.; Koretsky, G. M.; Gegenheimer, M.; Bergen, T.; Kappes, M. M. *Z. Phys. D*, in press.

(8) Goerke, A.; Leipelt, G.; Palm, H.; Schulz, C. P.; Hertel, I. V. *Z. Phys. D* **1995**, *32*, 311.

(9) Herschbach, D. *Faraday Discuss. Chem. Soc.* **1973**, *55*, 233.

(10) Lee, Y. T. *Science* **1987**, *263*, 793.

(11) Bewig, L.; Buck, U.; Mehlmann, C.; Winter, M. *J. Chem. Phys.* **1994**, *100*, 2765.

(12) Bewig, L.; Buck, U.; Gandhi, S. R.; Winter, M. *Rev. Sci. Instrum.* **1996**, *67*, 1.

(13) Würthwein, E.-U.; Schleyer, P. v. R.; Pople, J. A. *J. Am. Chem. Soc.* **1984**, *106*, 6973.

(14) Finocchi, F.; Noguera, C. *Phys. Rev. B*, in press.

(15) Mestdagh, J. M.; Balko, B. A.; Covinski, M. H.; Weiss, P. S.; Vernon, M. F.; Schmidt, H.; Lee, Y. T. *Faraday Discuss. Chem. Soc.* **1987**, *84*, 145.

(16) Weiss, P. S.; Covinski, M. H.; Schmidt, H.; Balko, B. A.; Lee, Y. T.; Mestdagh, J. M. *Z. Phys. D* **1988**, *10*, 227.

(17) Mestdagh, J. M.; Paillard, D.; Berlande, J. *J. Chem Phys.* **1988**, *88*, 2398.

(18) Buck, U.; Hoffmann, G.; Kesper, J.; Otten, D.; Winter, M. *Chem. Phys.* **1988**, *126*, 159.

(19) Bewig, L.; Buck, U.; Mehlmann, Ch.; Winter, M. *Rev. Sci. Instrum.* **1992**, *63*, 3936.

(20) Buck, U.; Ettischer, I.; Kreil, J.; Lauenstein, C. Unpublished results.

(21) Leipelt, G. Diplomarbeit, University Freiburg, 1993.

(22) Wright, T. G.; Ellis, A. M.; Dyke, J. M. *J. Chem. Phys.* **1993**, *98*, 2891.

(23) Levine, R. D.; Bernstein, R. B. *Molecular Reaction Dynamics and Chemical Reactivity*; Oxford University: New York, 1987.

(24) Grice, R. *Adv. Chem. Phys.* **1975**, *30*, 247.

(25) See ref 23, p 426.

(26) Poteau, R.; Spiegelman, F. *Phys. Rev. B* **1992**, *45*, 1878.

(27) Bonačić-Koutecky, V. Unpublished results.